IEEE Access
Multidisciplinary | Rapid Review | Open Access Journal

Received February 17, 2020, accepted April 28, 2020, date of publication May 4, 2020, date of current version May 19, 2020.

Digital Object Identifier 10.1109/ACCESS.2020.2992077

Coherent OTDR Using Flexible All-Digital Orthogonal Phase Code Pulse for Distributed Sensing

WENJIE CHEN, JUNFENG JIANG, KUN LIU, SHUANG WANG, ZHE MA, ZHENYANG DING, TIANHUA XU, AND TIEGEN LIU

School of Precision Instrument and Opto-electronics Engineering, Tianjin University, Tianjin 300072, China
Key Laboratory of Opto-electronics Information Technology, Tianjin University, Ministry of Education, Tianjin 300072, China
Tianjin Optical Fiber Sensing Engineering Center, Institute of Optical Fiber Sensing, Tianjin University, Tianjin 300072, China

Corresponding author: Junfeng Jiang (jiangjfjxu@tju.edu.cn)

This work was supported in part by the National Natural Science Foundation of China under Grant 61675152 and Grant 61735011, in part by the National Instrumentation Program of China under Grant 2013YQ030915, in part by the Tianjin Talent Development Special Plan for High Level Innovation and Entrepreneurship Team, and in part by the Open Project of the Key Laboratory of Opto-electronics Information Technology under Grant 2019KFKT007.

ABSTRACT A coherent optical time-domain reflectometer (COTDR) using flexible all-digital orthogonal phase code pulse is proposed for distributed acoustic sensing. All-digital orthogonal phase code pulse with frequency shift and time shift is used as probe. Coherent detection and balance photodetector are used to amplify interference signal and get rid of its direct-current (DC) component. The new scheme needs only single channel detection while keeping sampling frequency. Amplitude triangle modulation and frequency linear sweep modulation waveform are used for system performance investigation. The experiments on 15.4 km optical fiber showed that waveform information can be recovered well. The all-digital orthogonal phase code pulse will provide a flexible solution for different application requirement.

INDEX TERMS Optical fiber sensors, optical pulses, interference, phase detection, coherent OTDR, distributed sensing, phase extraction.

I. INTRODUCTION

Distributed acoustic sensing (DAS) system has a wide application on intrusion detection [1], seismic waves measurements [2], structure health monitoring [3] and pipeline monitoring [4], and so on. Comparing to optical frequency domain reflectometry (OFDR) [5]–[8], phase-sensitive optical time domain reflectometry (OTDR) based on Rayleigh backscattering (RBS) is a more common configuration for DAS. Quantitative waveform recovery requirement of DAS makes high performance phase extraction process play an important role to provide a linear response [9].

Phase extraction is usually realized with the phase generated carrier (PGC) [10], [11], the path-matched interferometry [12], and phase diversity detection [13], [14]. Among them, phase diversity detection is a promising DAS phase demodulation method for its ability to eliminate the common mode noise generated on the sensing fiber. A. Masoudi *et al.* used a 3 × 3 coupler to construct an unbalanced Michelson interferometer and output three interference signals with 120° phase shift in sequence [15]. J. Jiang *et al.* realized coherent phase diversity detection by utilizing a 3 × 3 coupler and pulse pair containing two pulses with difference frequency [16]. But the perturbation on the two arms of the interferometer may produce phase noise and reduce signal to noise ratio (SNR). The spatial resolution is also fixed by the optical path difference of interferometer arms. Three channels simultaneous high-speed detection also increase the system data acquisition hardware difficulty and cost. Z. Wang *et al.* reduce the simultaneous detection to two channels by utilizing a 90-degree hybrid, which realizes a 90° phase shift between two interference signals [17]. A. E. Alekseev *et al.* proposed a single-channel detection by combining an intensity modulator and a phase modulator to realize differential phase-shift keying modulation [18]. Three probe pulses are injected into the sensing fiber in sequence to

The associate editor coordinating the review of this manuscript and approving it for publication was Cesar Vargas-Rosales.

emulate analog phase diversity demodulation. The first part phase of pulses are zeros while the second part of pulses are delayed by relative phase shift $2\pi/3$.However, the obtained three interference signals are non-simultaneous detection and the acoustic-induced phase itself may vary between them. In addition, its measurement bandwidth is also reduced by 2/3. In order to overcome the problem of measurement bandwidth, A. E. Alekseev *et al.* then adapted a dual pulse and heterodyne detection method with each pulse having different carrier frequency [19]. The phase is demodulated through a I/Q quadrature demodulator with two analog harmonic radio signals. Experiment was demonstrated with PZT transducer being locating at the 1 km from the beginning of sensing fiber. X. He et al proposed a similar method with a digital I/Q quadrature demodulating algorithm [20]. They used two acousto-optic modulators and a delay fiber to generate heterodyne dual pulse. The demodulation experiment was demonstrated on 0.47 km sensing fiber and spatial resolution is fixed by the delay fiber. Y. Muanenda *et al.* combined the dual pulse with phase generated carrier technique [21]. They used an acousto-optic modulator, a phase modulator and a delay fiber to generate homodyne dual pulse. The demodulation experiment was demonstrated on 1 km sensing fiber and the 2kHz frequency vale information was retrieved correctly, however, the recovered waveform fidelity was low. Direct detection is adapted by the above dual-pulse-based phase extraction schemes. Thus, the sensing fiber length will be limited by weak backscattering signal. Y. Shan *et al.* combined ultra-weak fiber Bragg grating array (UWFBG) and distributed pump using a Raman fiber laser to enhance the light signal intensity, which helped the experiment demonstration on 42 km sensing fiber. However, the spatial resolution is fixed by the interval of UWFBG and prevents the possibility from using the dark optical fibers deployed for telecommunication.

In this paper, we proposed a coherent OTDR using flexible all-digital orthogonal phase code pulse for distributed sensing. We use a DPMZM to realize flexible all-digital orthogonal pulse with frequency shift and time shift. Coherent detection and balance photodetector are used to coherently amplify the RBS signals and get rid of the DC component of interference. The new scheme only needs a single channel detection while keeping sampling frequency. Orthogonal signals are obtained by digital mixing. We carried out experiment on 15.4 km sensing optical fiber with 10 m optical fiber wrapped on a piezoelectric ceramics (PZT). Modulation signals with amplitude triangle envelopment modulation and frequency linear sweep modulation are loaded on the PZT. The experiment results showed that applied modulation signal waveforms are recovered well. In addition, all-digital orthogonal phase code pulse provides a flexible solution for different requirements from potential applications, such as spatial resolution, signal intensity adjusting related with spatial interval, and so on.

II. PRINCIPLE

As shown in Fig. 1, the light is modulated into digital orthogonal phase code pulse, which is a triple-pulse contain three sub-pulses locating with frequency shift f_1, f_2 and f_3, and time shift W_0. The initial phases of the three sub-pulses are coded with 0°, 0° and 90°. The pulse width of the three sub-pulses are all W. The two sub-pulses with frequencies f_1 and f_3 emitted simultaneously while another sub-pulse with frequency f_2 emitted $W_0 + W$ earlier than them. The triple-pulses are emitted with T repetition time.

The triple-pulses can be generated with a dual parallel Mach-Zehnder modulator (DPMZM) driven by two voltage waveforms expressed as:

$$V_1(t) = V_D rect\left(\frac{t-W_0}{W}\right)\cos\left[2\pi f_2\left(t-W_0\right)\right] + V_D rect \times \left(\frac{t}{W}\right)\left[\cos\left(2\pi f_1 t\right) + \cos\left(2\pi f_3 t + 90°\right)\right] \quad (1)$$

$$V_2(t) = V_D rect\left(\frac{t-W_0}{W}\right)\sin\left[2\pi f_2\left(t-W_0\right)\right] + V_D rect \times \left(\frac{t}{W}\right)\left[\sin\left(2\pi f_1 t\right) + \sin\left(2\pi f_3 t + 90°\right)\right] \quad (2)$$

where V_D is the amplitude of the voltage signal which need be much less than the half-wave voltage V_π for linearly modulation [22]

The coherent detection scheme is shown in Fig. 2. The light with an optical frequency of f_0 from a narrowband continuous wave laser goes through a 1 × 2 fiber coupler. The light is divided into the local reference light and the signal light. The local reference light goes through a polarization controller and enters the 2 × 2 fiber coupler. The signal light goes into a

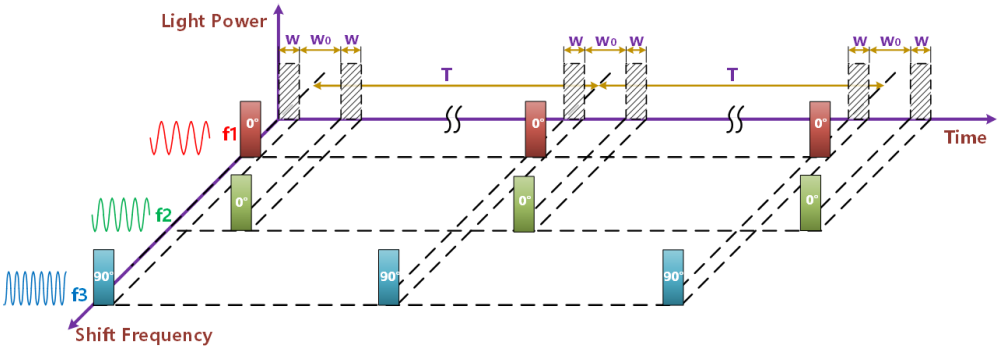

FIGURE 1. Scheme of all-digital orthogonal phase code pulse.

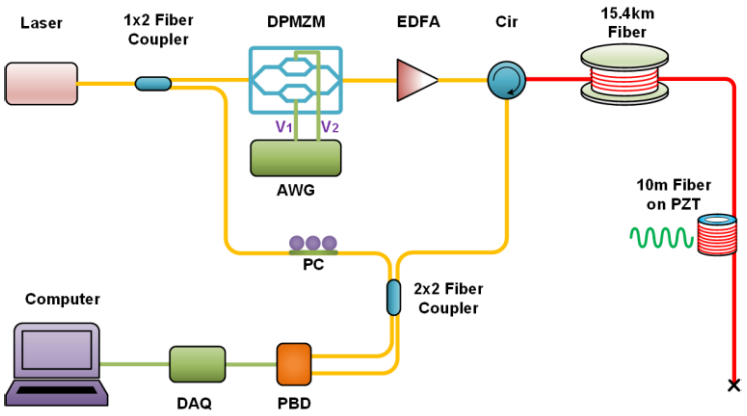

FIGURE 2. Scheme of coherent OTDR system using all-digital orthogonal phase code pulse.

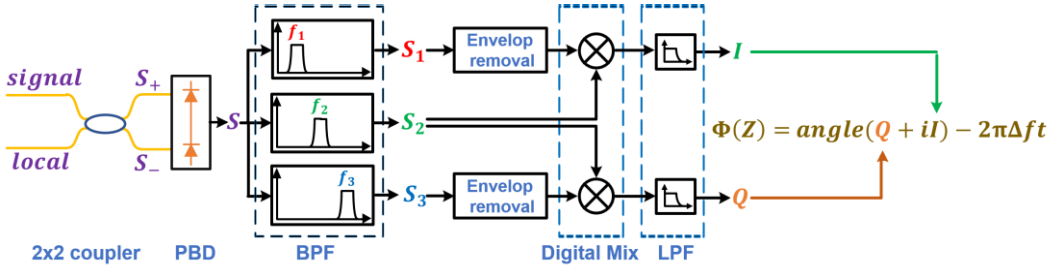

FIGURE 3. Diagram of phase demodulation algorithm.

DPMZM which is driven by an arbitrary waveform generator (AWG). The triple-pulses are generated and then amplified by the Erbium-doped fiber amplifier (EDFA). Then the amplified pulses are injected into the sensing fiber through the circulator. When the pulses are transmitted in the sensing fiber, the RBS is generated at each scattering points in the fiber. The generated RBS light comes back along the sensing fiber, goes through the circulator and interfere with the local reference light in the 2×2 fiber coupler. The interference light signals are received by the photoelectric balance detector (PBD) and transformed into electronical signal. DC component of interference signal is discarded by PBD and the alternating component is sent to the data acquisition (DAQ) card. The collected data is transmitted to the computer and processed.

The carrier frequencies of the interference signal are equal to the shift frequencies f_1, f_2 and f_3. And the phases of the coherent OTDR signals are the difference value between the phase corresponding to position of sensing fiber and the local reference fiber phase. Thus, the signal can be expressed as:

$$\begin{aligned} S = {} & A_1(t)\sin\left[2\pi f_1 t + \phi(Z) - \phi_{Loc}\right] \\ & + A_2(t)\sin\left[2\pi f_2 t + \phi(Z+L) - \phi_{Loc}\right] \\ & + A_3(t)\sin\left[2\pi f_3 t + \phi(Z) - \phi_{Loc} + 90^\circ\right] \end{aligned} \tag{3}$$

where, f_1, f_2 and f_3 are the carrier frequencies of the coherent OTDR signals, for simplifying we let $\Delta f = f_2 - f_1 = f_3 - f_2$. Z is the coordinate of the scattering point of sub-pulses with f_1 and f_3. ϕ_{Loc} is the phase of the local reference light. $\phi_1(Z)$, $\phi_2(Z+L)$, $\phi_3(Z)$ are the phase corresponding to the position Z and $Z+L$ on the sensing fiber. L is corresponding to the pulse interval W_0.

Fig. 3 shows the demodulation procedure. The signal is filtered by three bandpass filters to be decomposed into three signals:

$$S_1 = A_1(t)\sin\left[2\pi f_1 t + \phi(Z) - \phi_{Loc}\right] \tag{4}$$

$$S_2 = A_2(t)\sin\left[2\pi f_2 t + \phi(Z) - \phi_{Loc}\right] \tag{5}$$

$$S_3 = A_3(t)\sin\left[2\pi f_3 t + \phi(Z) - \phi_{Loc} + 90^\circ\right] \tag{6}$$

The envelopes of S_1 and S_3 are removed and the results are then mixed with S_2 respectively. The phase difference induced by frequency shift can be neglected since the shift frequency is far smaller than optical frequency. Therefore, the orthogonal signal I and Q can be obtained after the lowpass filters:

$$I = \frac{A_2(t)}{2}\cos\left[2\pi\,\Delta f t + \Phi(Z)\right] \tag{7}$$

$$Q = \frac{A_2(t)}{2}\cos\left[2\pi\,\Delta f t + \Phi(Z) + 90^\circ\right] \tag{8}$$

$$\Phi(Z) = \phi(Z+L) - \phi(Z) \approx \frac{4\pi}{\lambda} \bullet nL \tag{9}$$

where, n is the fiber effective refractive index; λ is the vacuum wavelength of the laser; $\Phi(Z)$ is the phase difference

corresponding to the distance L. $\Phi(Z)$ is extracted by finding the angel of complex number $Q + iI$ and minus $2\pi\,\Delta ft$.

When strain ε induced by acoustic event is applied to the fiber between the Z and $Z + L$ position point, tiny change in fiber length and fiber refractive index are introduced. The differential phase variation $\Delta\Phi(Z)$ is proportional to the strain ε by:

$$\Delta\Phi(Z) = \frac{4\pi L}{\lambda}\left\{n - \frac{n^3}{2}\left[p_{12} - \mu\left(p_{11} + p_{12}\right)\right]\right\} \bullet \varepsilon \qquad (10)$$

where μ the material Poisson's ratio; p_{11}, p_{12} are elements of elastic-optic coefficient matrix.

III. EXPERIMENTAL SETUP AND RESULTS

A. SYSTEM SETUP

We established experiment setup according to Fig.2. The narrowband laser generates CW light with 1550.12nm wavelength, less than 3kHz linewidth and 40mW output power. The bandwidth of DPMZM (Photoline MXIQ-LN-40) is 40GHz. The rise time of this modulator is less than 25ps, which is negligible compared to the light pulse width. The dual-channel arbitrary waveform generator (AT-AWG-GS 2500) has 14-bit vertical resolution, 2.5GS/s sampling rate. The frequency shift of the sub-pulses are set as $f_1 = 46MHz, f_2 = 65MHz$ and $f_3 = 84MHz$ for satisfied the effective spectrum range. The sub-pulse width is $W = 100ns$ and the interval time is $W_0 = 100ns$. The repeat period of digital orthogonal phase code pulse is $T = 200\mu s$. Thus, the sample rate of distributed sensing is 5kHz. A 10-meter fiber wrapped on a PZT is utilized for simulating the strain perturbation caused by acoustic field waveform. The 10-meter fiber is connected to the end of a 15.4km long optical fiber. A function waveform generator (Agilent33521A) generates voltage signals to drive the PZT. The working frequency range of the BPD is from 30kHz to 150MHz. And the data is sampled by a DAQ card with 1GS/s sampling rate and 12-bit resolution.

B. EXPERIMENTAL RESULTS

An amplitude modulation (AM) signal is applied to the 10-meter fiber. The carrier signal is a sinusoidal signal with fixed frequency of 200Hz and the amplitude of 1V.

The amplitude modulation signal is a triangular-wave with the frequency of 10Hz and the AM ratio of 10%∼100%, which changes the waveform amplitude from 0.1V to 1V.

Fig. 4(a) showed the spatial-temporal domain retrieving result. And an AM sinusoid waveform can be recognized at 15.4km. The location information and waveform of signal are detected correctly. The detail recovered waveform is shown in Fig. 4(b), the orange discrete points are the measured results and the green curve is the fitting curve of the retrieved waveform. The waveform is recovered well with fitting R-squared value 0.9939 and root mean squared error 0.0625. The zoomed local graph in Fig. 4(c) gives a more direct observation with retrieved signal waveform having little distortion. Fig.4(d) gives the power spectral density of recovered signal. The measured carrier frequency and the AM

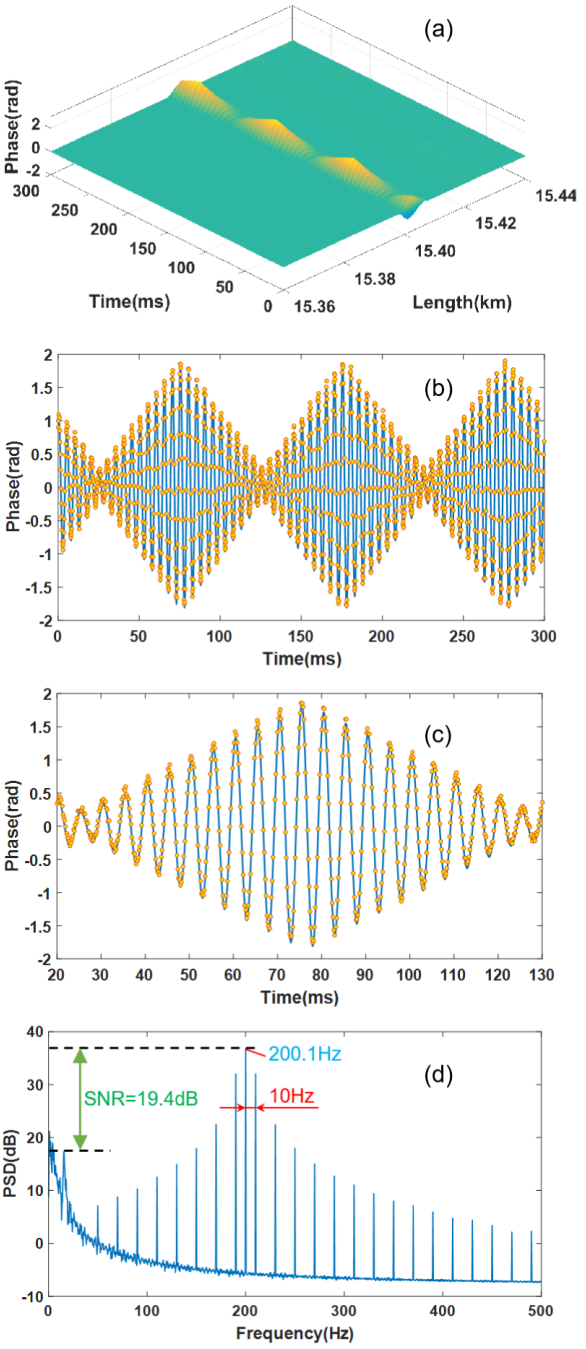

FIGURE 4. (a) 3D plot of spatial-temporal domain retrieved result of AM signal. (b) The retrieved waveform temporal domain curve at 15.40km from 0 to 300ms. (c) The partial enlargement graph of the temporal domain curve at 15.40km from 20 to 130ms. (d) PSD of the recovered signal.

frequency of the fitting curve are 200.1Hz and 10.0Hz, which are consistent with the loaded signal. The SNR achieves 19.4dB. The center frequency in the spectrum of the AM signal is the carrier frequency, while the space between this center line to the nearest lines on left or right is the AM frequency.

In the practical application scenario of distributed acoustic sensing, the acoustic frequency will provide important information for calculating the velocity of a moving sound source based on the sound Doppler effect. We then investigated frequency detection performance of the system A signal with fixed amplitude and linear frequency modulation is loaded to the sensing fiber. The fixed amplitude is 1V. The frequency sweep from 100Hz to 500Hz in 400ms linearly. The time-frequency analysis diagram of the retrieved waveform instant center frequency at 15.4km is shown in Fig. 5(a), from which obvious periodical frequency linear variation can be seen. The repetition period can be recognized as 400ms which is consistent with the signal loaded. The length of the hamming window used in short-time Fourier transform is 256 points while the step is 1 point. The measured center frequency and the fitting curving are showed in Fig5(b). The stepped increasing blue line shows the measured center frequency over time, while the red line shows the linear fitting curving. The interpolate frequency resolution 4.9Hz is limited by the Fourier transform length 1024 points when executing short-time Fourier transform. As shown in Figure 5(b), there are obvious deviations from the set frequency nearby the 100 Hz and 500Hz. The deviations from the set frequency nearby the 100 Hz and 500Hz are caused by the discontinuity between front part and end part of frequency sweeping cycles, i.e., when hamming window move to the location with frequency being round 100Hz or 500Hz, the discontinuous point exist in the intercepted window signal. Excluding the data in the front part and end part of the frequency sweeping cycles, the slope of calculated frequency sweep is ∼1001.3Hz/s, only deviated 1.3 Hz/s from set sweep slope 1000Hz/s. The experiment result shows that the linear scanning frequency signal can be well detected and recovered.

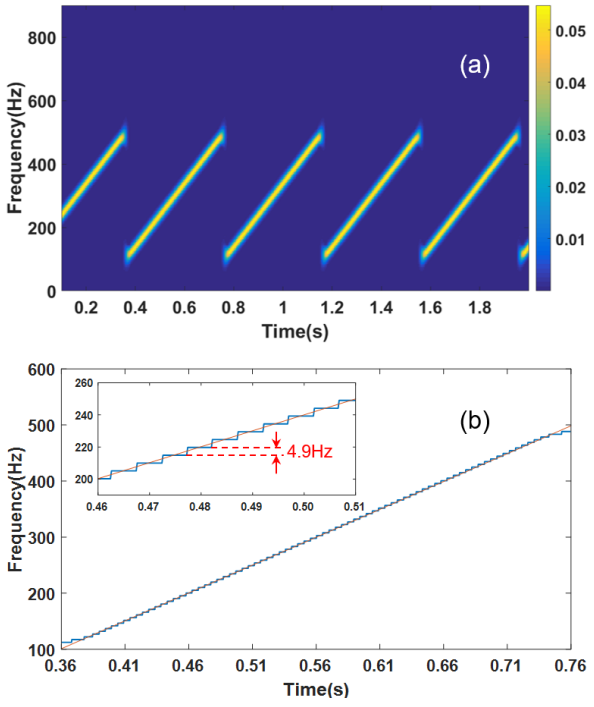

FIGURE 5. (a)Time-frequency analysis diagram 2D plot of the retrieved waveform instant center frequency; (b)Measured center frequency.

IV. CONCLUSION

A coherent OTDR using all-digital orthogonal phase code pulse is proposed and demonstrated for distributed acoustic sensing. We use a DPMZM to realize flexible all-digital orthogonal pulses with three different shift frequencies. Coherent detection and balance photodetector are used to coherently amplify the RBS signals and get rid of the DC component of interference. The new scheme only needs a single channel detection while keeping sampling frequency. Experiment are carried out on 15.4 km optical fiber. Amplitude triangle modulation and frequency linear sweep modulation waveform are used for system performance investigation. The experiment results showed that waveform information can be recovered well. The all-digital orthogonal phase code pulse can provide a flexible solution for different distributed acoustic sensing applications.

REFERENCES

[1] J. C. Juarez, E. W. Maier, K. Nam Choi, and H. F. Taylor, "Distributed fiber-optic intrusion sensor system," *J. Lightw. Technol.*, vol. 23, no. 6, pp. 2081–2087, Jun. 2005.

[2] K. N. Madsen, M. Thompson, T. Parker, and D. Finfer, "A VSP field trial using distributed acoustic sensing in a producing well in the North Sea," *1st Break*, vol. 31, no. 11, pp. 51–56, 2013.

[3] S. Dou, J. Ajo-Franklin, T. Daley, M. Robertson, T. Wood, B. Freifeld, R. Pevzner, J. Correa, K. Tertyshnikov, M. Urosevic, and B. Gurevich, "Surface orbital vibrator (SOV) and fiber-optic DAS: Field demonstration of economical, continuous-land seismic time-lapse monitoring from the Australian CO_2 CRC Otway site," in *Proc. SEG Tech. Program Expanded Abstr.*, Sep. 2016, pp. 5552–5556.

[4] J. Tejedor, J. Macias-Guarasa, H. Martins, D. Piote, J. Pastor-Graells, S. Martin-Lopez, P. Corredera, and M. Gonzalez-Herraez, "A novel fiber optic based surveillance system for prevention of pipeline integrity threats," *Sensors*, vol. 17, no. 2, p. 355, 2017.

[5] L. Xie, Z. Wang, J. Xiong, and Y. Rao, "Distributed acoustic sensing based on correlation analysis of fast and linear sweep OFDR," in *Proc. 16th Int. Conf. Opt. Commun. Netw. (ICOCN)*, Aug. 2017, pp. 1–3.

[6] Q. Liu, X. Fan, and Z. He, "Time-gated digital optical frequency domain reflectometry with 16-m spatial resolution over entire 110-km range," *Opt. Express*, vol. 23, no. 20, Oct. 2015, Art. no. 25988.

[7] B. Wang, X. Fan, S. Wang, G. Yang, Q. Liu, and Z. He, "Phase noise mitigation for long-range OFDR using ultrafast frequency sweep," in *Proc. Int. Conf. Photonics Switching*, 2016, pp. 1–3.

[8] E. Leviatan and A. Eyal, "High resolution DAS via sinusoidal frequency scan OFDR (SFS-OFDR)," *Opt. Express*, vol. 23, no. 26, p. 33318, Dec. 2015.

[9] H. F. Martins, S. Martin-Lopez, P. Corredera, M. L. Filograno, O. Frazao, and M. Gonzalez-Herraez, "Phase-sensitive optical time domain reflectometer assisted by first-order Raman amplification for distributed vibration sensing over >100 km," *J. Lightw. Technol.*, vol. 32, no. 8, pp. 1510–1518, Apr. 2014.

[10] A. Dandridge, A. B. Tveten, and T. G. Giallorenzi, "Homodyne demodulation scheme for fiber optic sensors using phase generated carrier," *IEEE Trans. Microw. Theory Techn.*, vol. 30, no. 10, pp. 1635–1641, Oct. 1982.

[11] K. Wang, M. Zhang, F. Duan, S. Xie, and Y. Liao, "Measurement of the phase shift between intensity and frequency modulations within DFB-LD and its influences on PGC demodulation in a fiber-optic sensor system," *Appl. Opt.*, vol. 52, no. 29, pp. 7194–7199, Oct. 2013.

[12] T. K. Lim, Y. Zhou, Y. Lin, Y. M. Yip, and Y. L. Lam, "Fiber optic acoustic hydrophone with double Mach–Zehnder interferometers for optical path length compensation," *Opt. Commun.*, vol. 159, nos. 4–6, pp. 301–308, Jan. 1999.

[13] E. Gottwald and J. Pietzsch, "Measurement method for determination of optical phase shifts in 3 × 3 fibre couplers," *Electron. Lett.*, vol. 24, no. 5, pp. 265–266, 1988.
[14] D. Chen, Q. Liu, and Z. He, "High-fidelity distributed fiber-optic acoustic sensor with fading noise suppressed and sub-meter spatial resolution," *Opt. Express*, vol. 26, no. 13, pp. 16138–16146, Jun. 2018.
[15] A. Masoudi and T. P. Newson, "High spatial resolution distributed optical fiber dynamic strain sensor with enhanced frequency and strain resolution," *Opt. Lett.*, vol. 42, no. 2, pp. 290–293, Jan. 2017.
[16] W. Chen, J. Jiang, S. Wang, K. Liu, Z. Ma, G. Liang, Z. Ding, Y. Zhang, P. Niu, and T. Liu, "Hybrid demodulation method for distributed acoustic sensing based on coherent detection and pulse pair," *Appl. Phys. Express*, vol. 13, no. 1, Jan. 2020, Art. no. 012012.
[17] Z. Wang, L. Zhang, S. Wang, N. Xue, F. Peng, and M. Fan, "Coherent ϕ-OTDR based on I/Q demodulation and homodyne detection," *Opt. Express*, vol. 24, no. 2, pp. 853–858, 2016.
[18] A. E. Alekseev, V. S. Vdovenko, B. G. Gorshkov, V. T. Potapov, I. A. Sergachev, and D. E. Simikin, "Phase-sensitive optical coherence reflectometer with differential phase-shift keying of probe pulses," *Quantum Electron.*, vol. 44, no. 10, pp. 965–969, Oct. 2014.
[19] A. E. Alekseev, V. S. Vdovenko, B. G. Gorshkov, V. T. Potapov, and D. E. Simikin, "A phase-sensitive optical time-domain reflectometer with dual-pulse diverse frequency probe signal," *Laser Phys.*, vol. 25, no. 6, Jun. 2015, Art. no. 065101.
[20] X. He, S. Xie, F. Liu, S. Cao, L. Gu, X. Zheng, and M. Zhang, "Multi-event waveform-retrieved distributed optical fiber acoustic sensor using dual-pulse heterodyne phase-sensitive OTDR," *Opt. Lett.*, vol. 42, no. 3, pp. 442–445, Feb. 2017.
[21] Y. Muanenda, S. Faralli, C. J. Oton, and F. Di Pasquale, "Dynamic phase extraction in a modulated double-pulse ϕ-OTDR sensor using a stable homodyne demodulation in direct detection," *Opt. Express*, vol. 26, no. 2, pp. 687–701, Jan. 2018.
[22] S. Gao and R. Hui, "Frequency-modulated continuous-wave lidar using I/Q modulator for simplified heterodyne detection," *Opt. Lett.*, vol. 37, no. 11, pp. 2022–2024, Jun. 2012.

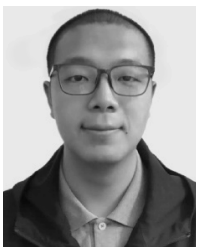

WENJIE CHEN is currently pursuing the Ph.D. degree in optical engineering with Tianjin University, Tianjin, China. His research interest includes distributed optical fiber sensing.

JUNFENG JIANG received the B.S. degree from the Southwest Institute of Technology, China, in 1998, and the M.S. and Ph.D. degrees from Tianjin University, Tianjin, China, in 2001 and 2004, respectively. He is currently an Associate Professor with Tianjin University. His research interests include fiber sensors and optical communication performance measurement.

KUN LIU received the B.Eng., M.Eng., and Ph.D. degrees from Tianjin University, Tianjin, China, in 2004, 2006, and 2009, respectively. He is currently an Associate Professor with Tianjin University. His research interests include fiber physics and chemistry sensing systems.

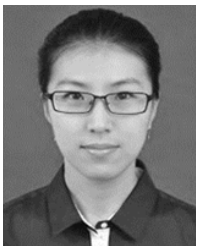

SHUANG WANG was born in Tianjin, China, in 1982. She received the B.S. degree from Shandong University, Shandong, China, in 2005, and the M.S. degree from Tianjin University, Tianjin, China, in 2007. She is currently a Lecturer with Tianjin University. Her research interests include optical fiber sensing and demodulation algorithm.

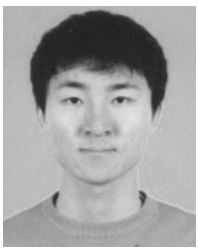

ZHE MA received the B.S. and M.S. degrees from the Taiyuan University of Technology, China, in 2012 and 2015, respectively. He is currently pursuing the Ph.D. degree in optical engineering with Tianjin University, Tianjin, China. His research interest includes distributed optical fiber sensing.

ZHENYANG DING received the B.S. degree in opto-electronics information engineering and the M.S. and Ph.D. degrees in optical engineering from Tianjin University, Tianjin, China, in 2008, 2010, and 2013, respectively. From 2013 to 2015, he was a Postdoctoral Researcher with the University of Maryland, College Park, MD, USA. He is currently an Associate Professor with the School of Precision Instruments and Optoelectronics Engineering, Tianjin University. His research interest includes optical coherence tomography.

TIANHUA XU received the B.Eng. and M.Eng. degrees from Tianjin University, Tianjin, China, in 2005 and 2008, respectively, and the Ph.D. degree from the KTH Royal Institute of Technology, Stockholm, Sweden, in 2012. He is currently a Professor with Tianjin University. His main research interests include fiber optic sensing and optical communication performance measurement.

TIEGEN LIU received the B.Eng., M. Eng., and Ph.D. degrees from Tianjin University, Tianjin, China, in 1982, 1987, and 1999, respectively. He is currently a Professor with Tianjin University. He is also a Chief Scientist with the National Basic Research Program of China. His research interests include photoelectric detection and fiber sensing.